



HAL
open science

Hexafluoroisopropanol-Induced Facial Selectivity in a Hindered Diels–Alder Reaction

David Kornfilt, Brian Chamberlain, Isabelle Chataigner, Riccardo Spezia, Florence Wagner

► **To cite this version:**

David Kornfilt, Brian Chamberlain, Isabelle Chataigner, Riccardo Spezia, Florence Wagner. Hexafluoroisopropanol-Induced Facial Selectivity in a Hindered Diels–Alder Reaction. *Synthesis: Journal of Synthetic Organic Chemistry*, 2023, 55 (13), pp.2047-2052. 10.1055/a-2016-4548 . hal-04225639

HAL Id: hal-04225639

<https://hal.science/hal-04225639>

Submitted on 3 Oct 2023

HAL is a multi-disciplinary open access archive for the deposit and dissemination of scientific research documents, whether they are published or not. The documents may come from teaching and research institutions in France or abroad, or from public or private research centers.

L'archive ouverte pluridisciplinaire **HAL**, est destinée au dépôt et à la diffusion de documents scientifiques de niveau recherche, publiés ou non, émanant des établissements d'enseignement et de recherche français ou étrangers, des laboratoires publics ou privés.

Hexafluoroisopropanol induced facial selectivity in a hindered Diels-Alder reaction

David J. P. Kornfilt^{1,4}, Brian T. Chamberlain^{1,4}, Isabelle Chataigner^{2,3}, Riccardo Spezia², Florence F. Wagner^{1,4}

¹Center for the Development of Therapeutics, Broad Institute of MIT and Harvard, 415 Main St, Cambridge, MA, USA
²Sorbonne Université, CNRS, Laboratoire de Chimie Théorique, LCT, 75005 Paris, France
³Normandie Université, UNIROUEN, CNRS, INSA Rouen, COBRA Laboratory, F-76000 Rouen, France, ⁴These authors contributed equally to the manuscript.

florence.f.wagner@gmail.com



Received:
Accepted:
Published online:
DOI:

Abstract BRD4780 is a small molecule that can selectively clear mutant MUC1-fs protein in mucin kidney disease models. Prior syntheses of BRD4780 were unsuitable for preparation on large scale. In this manuscript we describe HFIP as a unique solvent that allowed the key Diels-Alder reaction to proceed with >20:1 *endo* diastereoselectivity, enabling the kg-scale preparation of BRD4780 for further studies.

Key words Diels Alder, Nitroalkene, BRD4780, Mucin-1 Kidney Disease, HFIP

Diels-Alder reactions have long been an essential component of the chemist's toolbox for assembling complex bicyclic systems.¹ The concerted nature of the reaction allows for very high fidelity in the translation of stereochemical and geometrical information from reactants to products.¹ However, relative stereochemistry in the Diels-Alder remains difficult to control, and reactions of highly substituted systems can be particularly challenging due to decreased reactivity.¹ Moreover, for these systems, competition between the electronically favored *endo* approach and sterically favored *exo* approach often leads to poor selectivity.^{1,2} In this work we describe the use of hexafluoroisopropanol (HFIP), a fluorinated and strongly hydrogen bonding solvent, to effect a highly *endo*-selective Diels-Alder reaction between cyclopentadiene and a hindered dienophile under mild conditions, simultaneously forming a total of 4 stereocenters. The unique diastereoselectivity observed for HFIP in this reaction enabled the kilogram scale synthesis of BRD4780, a promising small molecule currently being investigated for the treatment of Mucin-1 Kidney Disease (MKD).³ BRD4780 was initially studied as a potential anti-hypertensive agent⁴ and was subsequently discovered, through screening of the Broad Institute's Drug Repurposing Hub⁵, to selectively remove a toxic frameshift Mucin 1 (fs-MUC1) protein in an *in vivo* mouse model of MKD, while leaving the wild type MUC1 unaffected in human immortalized epithelial cells and human kidney organoids.⁶ The described synthetic route to

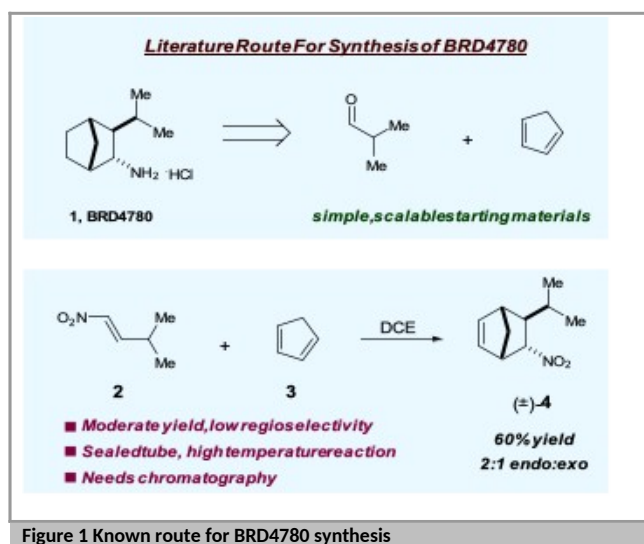


Figure 1 Known route for BRD4780 synthesis

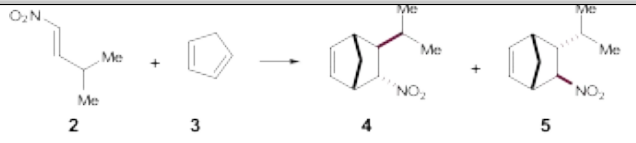
BRD4780 (Figure 1) proceeds through the Diels-Alder reaction of cyclopentadiene with (*E*)-nitroalkene **2** (prepared from isobutyraldehyde and nitromethane) to afford *endo*-norbornene **4** which is hydrogenated and converted into the HCl salt.⁴ This sequence, reported on a gram scale, is challenging to adapt to larger scale preparations because the key Diels-Alder step is conducted at high-temperature in a sealed tube and yields a significant amount of the undesired *exo* nitro product (*endo:exo* selectivity is 2:1) which, following hydrogenation, needs to be removed by careful silica gel chromatography. In the course of our studies, we needed to prepare large quantities of BRD4780 and therefore set out to optimize the Diels-Alder step. Ultimately, we report here an updated set of conditions which provide intermediate **4** with >20:1 diastereoselectivity without requiring sealed reaction vessels.

At the outset of the optimization campaign, we recognized the need to accurately quantify reagents and products analytically in each reaction. The low boiling points of **2** (67 °C at 18 mbar), **3** (41 °C at 1 bar) and cycloadduct **4** (76 - 80 °C at 3 mbar), as well as the water solubility of the latter, necessitated a detection

method that avoided extraction or concentration to avoid loss of components. Gas chromatography provided a convenient method that allowed for clean separation of reactants and products. We used both the observed *endo:exo* ratio as well as the mass balance in nitroalkene as figures of merit in comparing reaction conditions. Our initial solvent screen was designed to span a diverse space of physicochemical properties such as dielectric constant and hydrogen bonding ability. We first tested the previously reported Diels-Alder reaction conditions in 1,2-dichloroethane (DCE) and observed an *endo:exo* selectivity of 2.4:1, in line with literature precedent (Table 1, entry 1).⁴ Increasing solvent polarity only modestly affected the isomer ratio, whereas decreasing polarity had no effect (entries 2-6). Running the reaction in neat acetic acid did not greatly affect the outcome, whereas a stronger acid such as TFA resulted in decomposition (entries 7-8). Surprisingly, 2,2,2-Trifluoroethanol (TFE) increased the ratio of the *endo* product to 8:1, which was superior to other polar solvents (entry 9). This effect was even more dramatic with HFIP, where the highest *endo:exo* ratios were observed (> 14:1, entry 10).

Encouraged by this result, we focused on the concentration and temperature as key parameters (Table 2). We first evaluated concentration effects with toluene and found that dilution up to 20 V had minimal effect (entries 2-4). In contrast, dilution in TFE and HFIP had a substantially larger impact, with optimal results obtained at 20 V of solvent (entries 5-13), where no remaining starting material was detected after 18 h at 80 °C under these conditions. We also observed that, in HFIP, the total amount of *exo* product decreased substantially when the reaction was run at lower concentrations (entries 9-12). We selected 20 V for further evaluation based on diminishing returns. Gratifyingly, the *endo:exo* ratio did not decrease appreciably when the reaction was run with refluxing cyclopentadiene at 40 °C instead of in a sealed tube at 80 °C (entry 14). At this lower temperature, full conversion was only reached after extending the reaction time to 72 h (entries 8 and 15). The increase in reaction time was considered acceptable for pilot scale-up purposes due to an improved impurity profile and ease of operation. Under these optimized conditions, >90% conversion to the desired *endo* product could be achieved at 4.2 mmol scale.

Table 1. Effects of Solvent on Diastereoselectivity



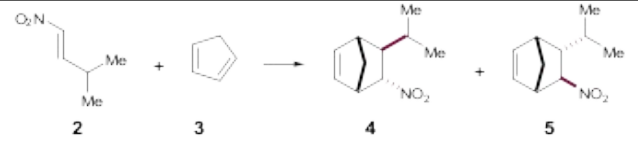
Entry ^a	Solvent	ϵ_s^b	4,% ^c	5,% ^c	Ratio
1	DCE	10.4	25.5	10.5	2.4
2	Toluene	2.4	15.2	7.9	1.9
3	THF	7.6	12.9	6.7	1.9
4	MeCN	37.5	30.5	10.9	2.8
5	DMF	36.7	20.9	8.1	2.6
6	MeOH	32.7	37.3	9.1	4.1
7	AcOH	6.2	33.9	10.6	3.2
8	TFA	8.6	0	0	N/A
9	TFE	8.6	37.0	4.7	7.9
10	HFIP	16.7	69.7	4.9	14.2

^aReactions run with 4.17 mmol **2**, 5 eq. **3**, 5 mL solvent at 80 °C for 18 h in sealed vials. See SI for full experimental details. ^bDielectric constant of solvent.

^cConversion determined by GC-MS against internal standard.

We next evaluated whether catalytic amounts of HFIP in DCE would be sufficient to replicate the effects. No increase in diastereoselectivity was obtained at different temperatures reaction was run at lower concentrations (entries 9-12). We selected 20 V for further evaluation based on diminishing returns. Gratifyingly, the *endo:exo* ratio did not decrease appreciably when the reaction was run with refluxing cyclopentadiene at 40 °C instead of in a sealed tube at 80 °C (entry 14). At this lower temperature, full conversion was only reached after extending the reaction time to 72 h (entries 8 and 15). The increase in reaction time was considered acceptable for pilot scale-up purposes due to an improved impurity profile and ease of operation. Under these optimized conditions, >90% conversion to the desired *endo* product could be achieved at 4.2 mmol scale when catalytic HFIP was employed (entries Table 3, entries 1-3). Other hydrogen-bonding and Lewis acid catalysts that have been reported to improve diastereoselectivity in analogous nitroalkene Diels-Alder reactions also did not recapitulate the effects of HFIP (entries 4-6).^{1, 7-8} Interestingly, thiourea **6** demonstrated marked acceleration and modestly improved selectivity in DCE. The additive effect of running the reaction in HFIP with catalysts was not explored in this study but may provide a path for further improvements. Notably, no Diels-Alder-type [4+2] products were detected when a catalytic quantity of SnCl₄ was introduced (entry 7, see SI for discussion of alternate mechanisms).⁹⁻¹¹

Table 2. Concentration and Temperature Screen



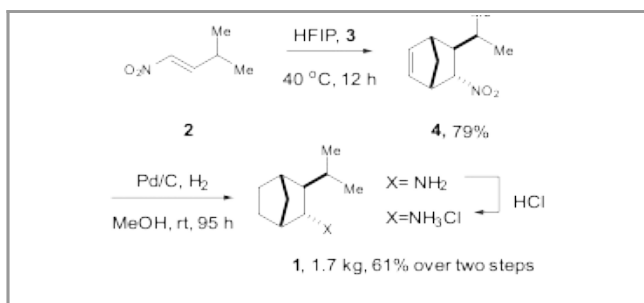
Entry ^a	Solvent	Conc., V	Temp., °C	4,% ^b	5,% ^b	Ratio 4:5
1	None	Neat	40	16.6	6.7	2.5
2	Tol	10	80	15.2	7.9	1.9
3	Tol	20	80	13.6	7.5	1.8
4	Tol	20	40	6.9	3.3	2.1
5	TFE	10	80	37.0	4.7	7.9
6	TFE	20	80	70.8	8.1	8.7
7	TFE	20	40	61.6	5.7	11
8	TFE	20	40 ^c	75.6	7.1	11
9	HFIP	1	80	54.3	8.2	6.6
10	HFIP	5	80	70.8	4.6	15
11	HFIP	10	80	69.7	4.9	14
12	HFIP	20	80	66.8	2.9	23
13	HFIP	40	80	46.7	2.7	17
14	HFIP	20	40	68.2	3.4	20
15	HFIP ^d	20	40 ^c	91.3	5.4	17

^aReactions run on 4.2 mmol scale, with 5eq. **3** in sealed vials for 18 h. See SI for full experimental details. ^bConversion determined by GC-MS against internal standard. ^cReaction time was 72 h. ^dAverage of two runs

Having established a dilute solution of HFIP at 40 °C as optimal conditions for yield and diastereoselectivity, we next proceeded with the scale-up of **4** on successively larger scales. Nitroalkene **2** was seen as a potential safety hazard due to the low molecular weight. DSC evaluation did not identify exothermic decomposition onset up to 150 °C and **2** was

deemed suitable for scale-up work (see SI). The preparation of nitroalkene **2** (Scheme 1) from the condensation of isobutyraldehyde and nitromethane proceeded smoothly, and 1.9 kg of **2** was prepared in a single batch. In the key Diels-Alder reaction, 1.3 kg of **2** was reacted with 5 equivalents of freshly cracked cyclopentadiene in 26.0 L of HFIP at 40 °C for 12 h. Notably, good conversion was achieved even within this shortened time frame. Work-up by extraction, washing and careful concentration in vacuo (boiling point of **4** is 76 - 80 °C @ 3 mbar) gave 2.7 kg of a crude oil with 55% w/w of the desired **4** by Q-NMR (74% yield). Gratifyingly, the *endo:exo* ratio was > 20:1 by GC analysis. This reaction was able to be reproduced with a second batch, affording 3.7 kg of oil with 50% w/w of desired **4** with >20:1 *endo:exo* (63% yield, 69% average across two runs). The total yield of key intermediate **4** was 33% compared to the literature yield of 12% from isobutyraldehyde. The crude **4** was hydrogenated with careful attention to completely remove partial hydrogenation byproducts such as hydroxylamines that may pose safety concerns. The hydrogenation of **4** across three separate hydrogenation campaigns followed by HCl salt formation and trituration with ethyl acetate furnished a total of 1.62 kg of the desired BRD4780 in 20% overall yield from purchased materials. Chromatography was not employed beyond the synthesis of **2**. In summary, the scale-up campaign was able to successfully deliver the required material for further testing and the key Diels-Alder step maintained the high diastereoselectivity that was achieved during the optimization process at kg-scale.

The unique nature of fluorinated solvents for pericyclic reactions has been well documented¹³⁻¹⁵, and we wished to rationalize the observed selectivity in the present case.



Scheme 1. Kg-scale synthesis of BRD4780

Although the *endo* product is favored in all the solvents tested, the imputed energy difference is small. Mutual steric repulsion between the bridging methylene of the cyclopentadiene and the isopropyl group appears to disfavor the *endo* configuration relative to nitroalkenes with smaller substituents at the β -position, which demonstrate higher *endo* selectivity.^{4,7} We first investigated whether the reaction was under kinetic or thermodynamic control by exposing purified *exo* product to the reaction solvents at 80 °C. No production of parent nitroalkene **2** or *endo* norbornene **5** was detected, confirming that the observed ratios were a result of kinetic selectivity (see SI). We therefore exclude the possibility of ground-state energy differences between the *endo* and the *exo* products governing the observed ratio. In conjunction with the previous results, we surmised that the increase in selectivity could stem from either a stabilization of the *endo* transition state, or a destabilization of the *exo* transition state driven by an interaction between the fluorinated, hydrogen bonding solvent and the nitro group. Therefore, we set out to calculate the relative energies of the potential transition states to gain a better insight into the underlying stereoelectronic factors.¹⁶

The transition state energies for both the *endo* and the *exo* pathways in various solvents were calculated using the M062X/6-31G(d,p)//M062X/Def2TZVPP method considering a polarized continuum (SMD) for the solvent effect (Table 4). Whereas the *exo* pathway is slightly favored in a vacuum (entry 1), the *endo* pathway becomes favorable upon solvation, as experimentally observed (entries 2-4). Furthermore, there is a small but significant correlation between solvent polarity and the observed transition state energies. However, as might be expected with the use of an implicit model for the solvent, the activation energy differences between **8** and **9** are only linked to the solvent polarity (compare entries 3 and 4) and these calculations failed to predict the improved selectivity in HFIP with respect to MeOH.

We next included an explicit molecule of solvent in each calculation to better compare MeOH and HFIP.¹⁷ The calculations revealed that the complex between the nitroalkene and the alcoholic solvent molecule in vacuum was tighter in the case of HFIP, with an O—H bond at 1.96 Å, while it is at 2.15 Å with MeOH, a trend that was maintained when implicit solvent fields were included (Table S1). The hydrogen bond activation is thus stronger in the case of HFIP, and in line with experiments, the activation energy was lower in HFIP compared to MeOH in

Table 3. Effect of Lewis Acid on selectivity



Entry ^a	Cat.	Temp	4, ^b %	5, ^b %	Ratio
1	HFIP	20	26	9	2.9
2	HFIP	40	26	8	3.3
3	HFIP	80	57	18	3.2
4	6	20	46	9	5.1
5	7	20	8	5	1.6
6	BF ₃ OEt ₂	20	5	0	N/A
7	SnCl ₄	20	0	0	N/A

^aReactions run on 4.2 mmol scale in sealed vials. See SI for full experimental details. ^bConversion determined by GC-MS against internal standard.

The diastereoselectivity of Diels-Alder reactions are known to be highly sensitive to solvent polarity.¹² However, in this case, the selectivity trend was not predicated on the dielectric constant (cf. Table 2). Furthermore, different classes of protic, aprotic, and polar solvents tested failed to significantly alter the selectivity. In contrast, TFE and HFIP, both of which are heavily fluorinated, provided some of the best selectivities observed.

the SMD vacuum framework (entries 5-6). The *endo* preference was also calculated in both cases using a SMD solvent continuum along with an explicit solvent molecule, however, once more the predicted *endo* preference was greater with MeOH (entries 7-8). Although the addition of a discrete molecule of solvent showed a stronger hydrogen bond activation of the nitroalkene in both cases compared to the implicit solvent model alone, the improved diastereoselectivity in HFIP with respect to MeOH was not apparent. Solvation properties were also investigated through classical molecular dynamics simulations. Although solvent accessible surface area analysis proved unfruitful, strengthening of a H-bonding network around the different TS structures was observed (SI, Table S2). In particular, such simulations clearly show that HFIP is much strongly structured around the nitro-group of the dienophile with respect to MeOH (Table S3 and Figure S6). How this property directly relates to observed improved diastereoselectivity in HFIP is not clear at the present time and merits more extensive calculations and specific computational studies. We also considered an alternative two-step pathway comprising an initial inverse electron demand Diels-Alder reaction to afford a cyclic nitronate followed by a [3,3]-sigmatropic rearrangement that could lead to the product, however this pathway was not considered probable based on both computational and experimental results (Table 3, entry 7 and Scheme S1).

Table 4 . Endo and Exo TS geometry at 298K

		 Endo TS 8		 Exo TS 9			
Entry	Medium	ϵ	$\Delta G^\ddagger_{\text{exo}}^a$	$\Delta G^\ddagger_{\text{endo}}^a$	$\Delta\Delta G^\ddagger^b$	Pred. d.r.	Actual d.r.
1	Vacuum	0	29.4	29.7	0.3	0.6	N/A
2	DCE	10.5	30.9	30.2	-0.7	3.0	2.4
3	HFIP	15.7	28.7	27.1	-1.6	14.4	14.2
4	MeOH	32.0	27.5	25.5	-2.0	29.3	4.1
5	HFIP/Vac ^c	0	30.3	31.3	-1.0	5.4	N/A
6	MeOH/Vac ^c	10.5	33.7	33.6	0.1	0.8	N/A
7	HFIP/HFIP ^c	15.7	24.5	26.9	-2.4	57.6	14.2
8	MeOH/MeOH ^c	32.0	27.3	30.0	-2.7	95.6	4.1

^aActivation energies were determined at the M062X/ def2-TZVPP/SMD (medium) level (single points calculations after an optimization of the geometries at the M062X/6-31G(d,p)/SMD (medium) level, as differences between the calculated energies of the TS and the separated substrates. ^bAll DG values are given in kcal/mol. ^cExplicit/implicit solvent used for calculations

Solvent choice is a key determinant of reaction outcome in pericyclic processes. In the present case, we were able to take advantage of the polar, fluorinated nature of HFIP to enable the diastereoselective and *endo*-stereoselective kg-scale synthesis of a key intermediate for BRD4780. The new process avoids the poor diastereoselectivity of the earlier process and obviates the

need for a high temperature sealed-tube reaction and chromatographic separation. Key mechanistic experiments and calculation of transition state energies allowed us to rule out some potential explanations for the high selectivity, and our efforts to characterize this phenomenon will be shared in due course.

The experimental section has no title; please leave this line here.

Isobutyraldehyde (78-84-2, 99%), nitromethane (75-52-5, 99%) and cyclopentadiene (542-92-7, 95%) were purchased from commercial sources and used as received. NMRs were acquired on a 400 MHz Bruker instrument. GC data were acquired on a Shimadzu GC2030 with an Agilent J&W HP-5MS column (30m x 0.25mm ID x 0.25 um film thickness). The acquisition method used N2 as a carrier gas (1.5 mL/min), an injector temp. of 250 °C, and a gradient ramp from 100 °C to 250 °C at 10 °C/min. For chiral GC analysis, an Agilent J&W CYCLOSIL-B (30 m x 0.25 mm ID x 0.25 μm film) column was used with a flow rate of 0.8 mL/min, He carrier gas, makeup flow of 30 mL/min, H2 flow of 40 mL/min and airflow of 400 mL/min. An isocratic temperature of 120 °C for 30min was used. SFC analyses were performed on an Agilent 1200 system with a Chiralpak AD-3 column (150mm x 4.6 mm) using a mobile phase of sCO₂ (A) and 0.1%IPA in MeOH (B). The gradient was from 90:10 A:B to 50:50 A:B over 3 min at a flow rate of 2.5 mL/min.

Procedure for kg-scale preparation of BRD4780-HCl (1)

Step 1: To a stirred solution of isobutyraldehyde (2.50 kg, 34.7 mol, 1.00 eq) and CH₃NO₂ (2.12 kg, 34.7 mol, 1.00 eq) in MeOH (12.5 L) in a 50 L round-bottom reactor with mechanical stirrer was added a solution of NaOH (1.66 kg, 41.6 mol, 1.20 eq) in H₂O (2.50 L) dropwise by dropping funnel (416 mL/h over 6 h) while the temperature was maintained between -1 and 1 °C. After addition, the reaction was slowly warmed to 20 °C over 3 hrs. The reaction was then stirred (350 RPM) at 20 °C for 12 hrs. TLC (Petroleum ether/EtOAc = 3/1, R_f = 0.60, KMnO₄) indicated isobutyraldehyde was consumed completely. Water (15.0 L) was added in one portion and the temperature was lowered from 23 °C to 20 °C and the mixture turned into a clear solution. The clear solution was then slowly added into a solution of 6 M HCl (40.0 L) by a peristaltic pump (addition speed is 8.00 L/h) while the temperature was maintained under 25 °C. After the addition was complete, the resulting mixture was stirred for 15 min. Then, the aqueous layer was extracted with DCM (15.0 L x 3). The combined organic was dried over anhydrous Na₂SO₄ (3.00 kg), filtered and concentrated. Q-NMR with 1,3,5-Trimethoxybenzene as a standard indicated the crude purity of **2** is 57.6%. The residue was purified by column chromatography (SiO₂ (10.0 kg, 200-300 mesh), Petroleum ether/EtOAc = 1000/1 to 1/1, total ~80 L of fraction), the column fractions were concentrated at 30 °C under vacuum (-0.08 Mpa to -0.10 Mpa), and the evaporated solvent was re-concentrated. The products were combined to afford **2** (1.90 kg, 47.6% yield) as a yellow oil with GCAP of 79%. ¹H NMR spectra were consistent with literature reports. The material was taken forward without further manipulation.

Step 2: Cyclopenta-1,3-diene was freshly cracked by distillation at 220 °C in a 5L 3-neck flask and the fraction boiling at 145-148 °C was collected in one portion over 5 h. To the crude solution of **2** (1.89 kg, 16.42 mol, 1.00 eq, 79% GCAP) in HFIP (30 L) in a 50 L round-bottom reactor equipped with a mechanical stirrer was added freshly cracked cyclopenta-1,3-diene (5.43 kg, 82.1 mol, 5.00 eq). The reaction was stirred at 200 RPM and 40 °C for 12 hrs. Analysis by TLC (Petroleum ether/EtOAc = 10/1, R_f = 0.65, PMA) showed that starting material was consumed, and GC analysis showed the *endo:exo* ratio was >20:1 (small impurities prevent determination of an exact ratio by this method). The mixture was cooled to 25 °C, and then poured into ice-water (w/w = 1/1) (15.0 L). A rise in temperature to 28 °C was observed. The aqueous phase was extracted twice with EtOAc (10.0 L for the first round, 5.00 L for the second round). The combined organic phase was washed with brine (8.00 L), dried with anhydrous Na₂SO₄ (800 g), filtered and concentrated in vacuum at 40 °C. Because of the low boiling point of **4**, the evaporated solvent was analyzed by TLC and almost no **4** was

detected. Compound **4** (3.70 kg, crude, ~50% purity by Q-NMR, 79% yield) was obtained as a yellow oil and characterized by ¹H NMR. Spectra were consistent with literature reports. The material was taken on to the next step without further manipulation.

Step 3: The reaction was run three times on 1.5-, 1.6- and 2.1-kg scale in two separate campaigns and showed some variability. A representative procedure is shown below:

Crude **4** (1.5 kg, ~50% QNMR purity) was distributed across two 10L autoclaves. To each solution of **4** (700 g and 800 g, 2.12 and 2.43 mol 1.00 eq) in MeOH (7.00 and 8.00 L) in 10 L autoclave was added Pd/C (240 g, 10% w/w on carbon) under Ar. The suspension was degassed under vacuum and purged with H₂ for three times. The mixture was stirred under H₂ (50 psi) at 25 °C for 47 hrs. (Note: the H₂ is replenished every 0.5 h during daytime based on safety guidelines). An aliquot for analytical characterization was filtered and injected into a GC system. The IPC spectra indicated the reaction was not complete as an intermediate species was observed. The temperature was raised to 30 °C and the reaction time was extended a further 48 h. A GC aliquot taken at this time showed that the reaction was complete. The reactions were combined for work up. The reaction mixture was filtered through celite (1000 g) and the filter cake was washed with MeOH (15.0 L), TLC (DCM/MeOH = 10/1, R_f = 0.20, KMnO₄) showed that no product remained in celite filter cake. Then HCl/EtOAc (4 M, 3.00 L) was added directly to the filtrate and the filtrate was concentrated in vacuum at 40 °C to give the crude product (2.00 kg) as a slurry. The residue was suspended with EtOAc (2.00 L), and stirred for 1 h at 15 °C, then filtered and the filter cake was washed with EtOAc (800 mL). The filter cake was then collected and dried under vacuum at 40 °C to give **BRD4780-HCl** (**1**, 650 g, 3.43 mol, 75.4%) yield as a white solid.

In separate campaigns, the procedure was repeated with 1.6 kg and 2.1 kg batches of **4** with ~50% QNMR purity (the 2.1-kg batch was split into 3 reactions of 700 g each) affording respectively 450 and 600 g of **BRD4780-HCl**. The combined material was suspended with MTBE (2.00 L), and stirred for 0.5 h at room temperature, then filtered and washed the filter cake with MTBE (800 mL), the filter cake was collected and dried under vacuum at 40 °C to give pure **BRD4780-HCl** (1020 g, 5.98 mol, 52.7% combined yield) as a white solid. Spectra were consistent with literature reports.⁴ Further work is necessary to understand the variability in the hydrogenation process. Average yield across the three campaigns was 60.9%.

Funding Information

This work was funded by the Slim Initiative for Genomic Medicine in the Americas (SIGMA), a collaboration of the Broad Institute with the Carlos Slim Foundation. Criann (Saint Etienne du Rouvray, France) is kindly acknowledged for allocation of computer time.

Acknowledgment

The authors thank Dr. Ludovic Decultot for determining the boiling points, Liang Sun, Hailiang Zhang, and co-workers (Wuxi, Tianjin) for executing the scale-up synthesis and Dr. Zhigang Li, Dr. Xun Lu, and co-workers (Shanghai Medicilon) for synthetic chemistry support and analytical method development.

Supporting Information

YES (this text will be updated with links prior to publication)

Primary Data

NO.

Conflict of Interest

Brian Chamberlain and Florence Wagner are named as inventors on pending PCT Application Serial Number PCT/US2021/065049, filed on December 23, 2021 and entitled "COMPOSITIONS AND METHODS RELATED TO BICYCLO[2.2.1] HEPTANAMINE-CONTAINING COMPOUNDS", which is owed by The Broad Institute and Instituto Carlos Slim de la Salud, A.C. (Mexico).

References

- (1) (a) Hubbard, R. D.; Miller, B. L. *J. Org. Chem.* **1998**, *63*, 4143-4146; (b) Nicolaou, K. C.; Snyder, S. A.; Montagnon, T.; Vassilikogiannakis, G. *Angew. Chem. Int. Ed.* **2002**, *41*, 1668-1698; (c) Corey, E. J.; Guzman-Perez, A. *Angew. Chem. Int. Ed.* **1998**, *37*, 388-401.
- (2) Lam, Y.-h.; Cheong, P. H.-Y.; Blasco Mata, J. M.; Stanway, S. J.; Gouverneur, V.; Houk, K. N. *J. Am. Chem. Soc.* **2009**, *131*, 1947-1957.
- (3) Dvela-Levitt, M.; Shaw, J. L.; Greka, A. *Trends Mol. Med.* **2021**, *27*, 394-409.
- (4) Munk, S. A.; Lai, R. K.; Burke, J. E.; Arasasingham, P. N.; Kharlamb, A. B.; Manlapaz, C. A.; Padillo, E. U.; Wijono, M. K.; Hasson, D. W.; Wheeler, L. A.; Garst, M. E. *J. Med. Chem.* **1996**, *39*, 1193-1995.
- (5) Corsello, S. M.; Bittker, J. A.; Liu, Z.; Gould, J.; McCarren, P.; Hirschman, J. E.; Johnston, S. E.; Vrcic, A.; Wong, B.; Khan, M.; Asiedu, J.; Narayan, R.; Mader, C. C.; Subramanian, A.; Golub, T. R. *Nat. Med.* **2017**, *23*, 405-408.
- (6) Dvela-Levitt, M.; Kost-Alimova, M.; Emani, M.; Kohnert, E.; Thompson, R.; Sidhom, E. H.; Rivadeneira, A.; Sahakian, N.; Roignot, J.; Papagregoriou, G.; Montesinos, M. S.; Clark, A. R.; McKinney, D.; Gutierrez, J.; Roth, M.; Ronco, L.; Elonga, E.; Carter, T. A.; Gnirke, A.; Melanson, M.; Hartland, K.; Wiedner, N.; Hsu, J. C.; Deltas, C.; Hughey, R.; Bleyer, A. J.; Kmoch, S.; Živná, M.; Barešova, V.; Kota, S.; Schlondorff, J.; Heiman, M.; Alper, S. L.; Wagner, F.; Weins, A.; Golub, T. R.; Lander, E. S.; Greka, A. *Cell* **2019**, *178*, 521-535.e23.
- (7) Takenaka, N.; Sarangthem, R. S.; Seerla, S. K. *Org. Lett.* **2007**, *9*, 2819-2822.
- (8) Wittkopp, A.; Schreiner, P. R. *Chem. Eur. J.* **2003**, *9*, 407-414.
- (9) Denmark, S. E.; Cramer, C. J.; Sternberg, J. A. *Helv. Chim. Acta* **1986**, *69*, 1971-1989.
- (10) Denmark, S. E.; Moon, Y. C.; Senanayake, C. B. W. *J. Am. Chem. Soc.* **1990**, *112*, 311-315.
- (11) Çelebi-Ölçüm, N.; Ess, D. H.; Aviyente, V.; Houk, K. N. *J. Am. Chem. Soc.* **2007**, *129*, 4528-4529.
- (12) Ruiz-Lopez, M. F.; Assfeld, X.; Garcia, J. I.; Mayoral, J. A.; Salvatella, L. *J. Am. Chem. Soc.* **1993**, *115*, 8780-8787.
- (13) Cativiela, C.; García, J. I.; Mayoral, J. A.; Salvatella, L. *Can. J. Chem.* **1994**, *72*, 308-311.
- (14) Cativiela, C.; I. García, J.; Gil, J.; M. Martínez, R.; A. Mayoral, J.; Salvatella, L.; S. Urieta, J.; M. Mainar, A.; H. Abraham, M. *J. Chem. Soc., Perkin Trans. 2* **1997**, 653-660.
- (15) Motiwala, H. F.; Armaly, A. M.; Cacioppo, J. G.; Coombs, T. C.; Koehn, K. R. K.; Norwood, V. M. I. V.; Aubé, J. *Chem. Rev.* **2022**, *122*, 12544-12747.
- (16) Jasiński, R.; Koifman, O.; Barański, A. *Open Chem.* **2011**, *9*, 1008-1018.
- (17) Yang, Y.-F.; Yu, P.; Houk, K. N., *J. Am. Chem. Soc.* **2017**, *139*, 18213-18221.